DOI: 10.1002/ejoc.200600921

Comparison between the Photophysical Properties of Pyrazolo- and Isoxazolo[60]fullerenes with Dual Donors (Ferrocene, Aniline and Alkoxyphenyl)

Laura Perez,[a] Mohamed E. El-Khouly,[b,c] Pilar de la Cruz,[a] Yasuyuki Araki,[b] Osamu Ito,*[b] and Fernando Langa*[a]

Keywords: Fullerenes / Electron transfer / Dual-donor–C_{60} systems / Electrochemistry / Laser spectroscopy

Two series of new pyrazolo- and isoxazolo[60]fullerenes covalently linked to vinylenephenylene bearing ferrocene, dibutylaniline or dodecyloxyphenyl electron-donor groups attached in the periphery have been synthesized. The photophysical properties of these newly synthesized dual-donor–C_{60} derivatives have been investigated and compared by applying time-resolved fluorescence and nanosecond transient techniques in both polar and nonpolar solvents. Charge separation via the excited singlet state of C_{60} is more efficient in the pyrazolo-C_{60} triads than in the isoxazolo-C_{60} triads. It was found that the pyrazoline ring mediates charge separation as a result of the stronger electron-donating character of the nitrogen atom of the pyrazoline ring compared with the oxygen atom of the isoxazoline ring.

Introduction

The construction of artificial photosynthetic models to mimic natural photosynthesis through the design of covalently linked electron-donor and -acceptor moieties is an area of great interest. The interest lies in the development of efficient organic solar cells[1] and other areas of nanotechnology such as photonics or sensors.[2] In this respect, fullerene C_{60} is an attractive core owing to its easy chemical functionalization which allows the incorporation of most functional groups.[3] Moreover, C_{60} is an excellent electron acceptor,[4] for example, its acceptor ability is similar to that of quinones, and its visible-light absorption allows efficient photoinduced events such as energy transfer (EN) and electron transfer (ET) in fullerene–donor dyads.[5] These systems can undergo efficient photoinduced electron-transfer (PET) processes to give long-lived radical-ion pairs.[2]

One crucial factor in donor–acceptor systems is light-harvesting. Dendrimer-based light-harvesting structures have received increased attention in recent years.[6] Some fullero-pyrrolidine derivatives substituted with multi-oligophenylenevinylene (OPV) moieties have provided very efficient photoinduced energy transfer from OPV to C_{60}.[7]

The donor ability of peripheral groups determines the nature of photophysical events in these systems; alkoxy groups only drive energy transfer,[8] but stronger donors in the periphery (e.g., multi-dibutylaniline[9] and multi-ferrocene units[10]) allow efficient electron transfer that generates the radical-ion pair.

The above-mentioned fullero-dendrimers have been prepared by 1,3-dipolar cycloaddition of azomethine ylides to C_{60}.[11] It is well known that fulleropyrrolidines exhibit a decrease in electron affinity with respect to the parent C_{60} owing to the saturation of one double bond. Nevertheless, fullerene derivatives in which a heteroatom (nitrogen or oxygen) is directly linked to the C_{60} cage, for example, isoxazolo-fullerenes (OxC_{60})[12] and pyrazolo-fullerenes (PzC_{60}),[13] exhibit similar or even higher electron-accepting ability than C_{60} as a result of the inductive effect of the heteroatom.

Although photophysical events in pyrrolo[60]fullerene derivatives are well known,[14] there have been very few detailed photophysical studies of OxC_{60}[12] and PzC_{60} derivatives[13] as donor–acceptor systems. These systems show different and more complex behaviour than pyrrolo[60]fullerene-based dyads.

PzC_{60} derivatives have recently been used to link electroactive groups to the C_{60} cage and the products show efficient PET processes.[15] It has been shown that the lone-pair electron of the pyrazoline sp^3 nitrogen atom is able to afford PET to the C_{60} cage.[7c] Thus, the Pz moiety acts as

[a] Facultad de Ciencias del Medio Ambiente, Universidad de Castilla-La Mancha,
45071 Toledo, Spain
Fax: +34-925-268-840
E-mail: Fernando.LPuente@uclm.es
[b] Institute of Multidisciplinary Research for Advanced Materials, Tohoku University,
Katahira, Aoba-ku, Sendai, 980-8577, Japan
Fax: +81-22-217-5608
E-mail: ito@tagen.tohoku.ac.jp
[c] Department of Chemistry, Faculty of Education, Kafr El-Sheikh, Tanta University,
Tanta, Egypt
E-mail: mohamedelkhouly@yahoo.com

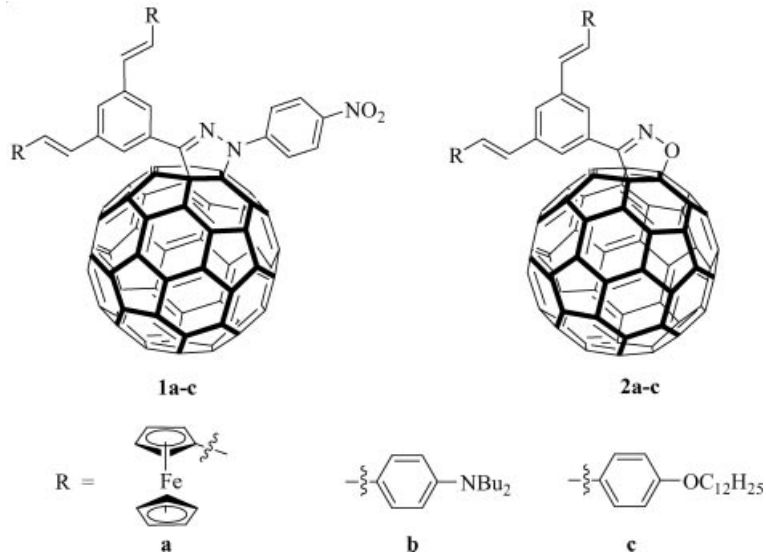

Figure 1. Pyrazolo- and isoxazolo[60]fullerenes systems.

an intermediary in the PET process from a donor unit present in the organic addend.[16] Interestingly, recent studies on organic photovoltaic cells[17] constructed with donor polymers and fullerene derivatives as acceptors indicate that cells built with PzC_{60} derivatives have a higher efficiency than those constructed with PCBM, highlighting the interest of these compounds.

We present herein the synthesis, electrochemistry and the first comparative study of the photophysical properties of two series of pyrazolo- (**1a**–**c**) and isoxazolo-fullerene (**2a**–**c**) derivatives in which three different kinds of donors {3,5-bis(2′-ferrocenylvinyl)phenyl [$(FcV)_2Ph$], 3,5-bis[2′-(4′-dibutylaminophenyl)vinyl]phenyl [$(R_2NPhV)_2Ph$] and 3,5-bis[2′-(4′-dodecyloxyphenyl)vinyl]phenyl [$(ROPhV)_2Ph$]} are linked to the C_{60} cage, as shown in Figure 1.

Results and Discussion

Synthesis and Characterization

The target pyrazolo[60]fullerenes **1a**–**c** were synthesized from the corresponding hydrazones **4a**–**c**[13a] (Scheme 1); the synthetic strategy was based on a 1,3-dipolar cycloaddition reaction between C_{60} and nitrile imines.

Hydrazones **4a**–**c** were prepared in good yields (65–90%) by the reaction of aldehydes **3a**–**c**[10,18] with 4-nitrophenylhydrazine in refluxing EtOH.[19] Two different procedures were used for the preparation of pyrazolo-fullerenes **1a**–**c**. Derivatives **1a** and **1b** were obtained (in 19 and 15% yields, respectively) by the reaction of **4a** and **4b** with *N*-chlorosuccinimide (NCS) in $CHCl_3$ at 0 °C and subsequent addition

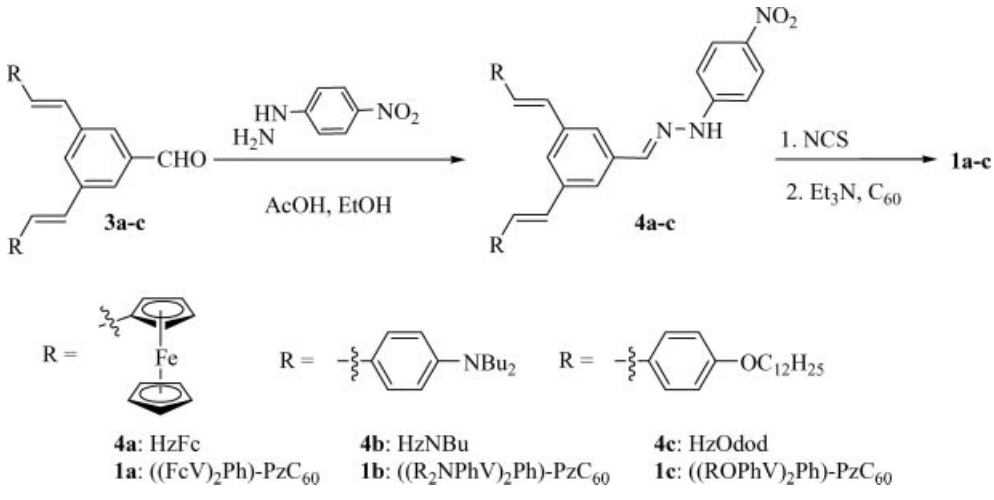

Scheme 1.

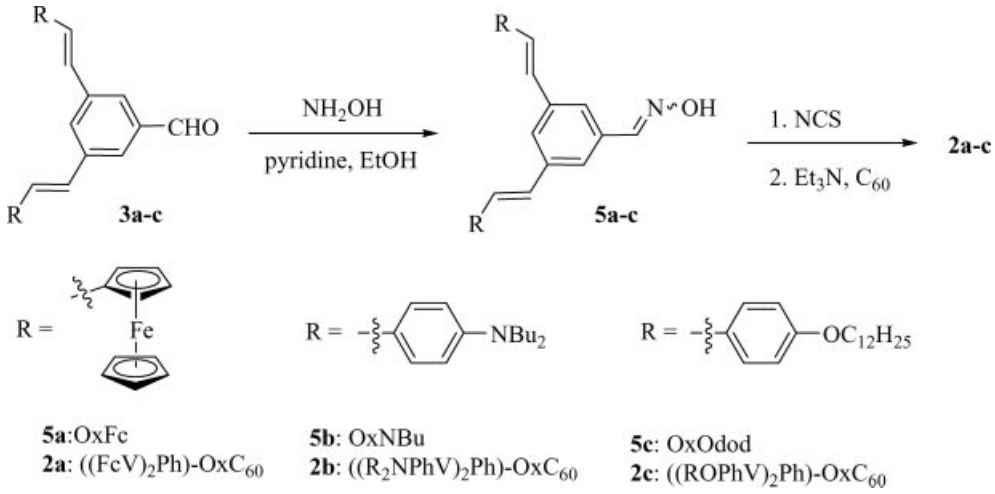

Scheme 2.

of C_{60} and Et_3N in toluene at room temperature to afford cycloadducts **1a** and **1b**. A similar procedure was used to prepare dyad **1c**, but the best yield (31%) was obtained by using microwave irradiation[20] at 210 W for 20 min after the addition of C_{60}. Finally, compounds **1a**–**c** were purified by flash chromatography.

The structures of the hydrazones **4a**–**c** and dyads **1a**–**c** were confirmed from their analytical and spectroscopic data (i.e., UV/Vis, FTIR, ^1H and ^{13}C NMR, and MALDI mass spectra). The ^1H NMR spectra of dyads **1a**–**c** exhibit the expected features with the correct integration ratios. Note that in all cases the protons of the vinyl systems appear as two ABq systems at around 6.90 and 7.05 ppm with coupling constants in the range J = 16–17 Hz, which shows that the stereochemistry of the double bonds corresponds to the (*E*) isomers. The structures of dyads **1a**–**c** were also confirmed by their MALDI-TOF mass spectra which show the expected M^+ peaks at m/z = 1379.1 (**1a**), 1417.4 (**1b**) and 1531.2 (**1c**), matching the calculated molecular weights.

Isoxazolo[60]fullerene systems (**2a**–**c**) were synthesized according to Scheme 2 by 1,3-dipolar cycloaddition of the corresponding nitrile oxide to C_{60}.[12a] The oximes **5a**–**c**, prepared in 89–99% yields from aldehydes **3a**–**c** according to the general procedure,[19] were treated with NCS in chloroform. The resulting products were reacted in situ with C_{60} and triethylamine in toluene at 0 °C for 2 h for compound **2a**, at room temperature for 2.5 h for compound **2b** and under focused microwave irradiation (210 W, 40 min) for compound **2c**. Compounds **2a**–**c** were obtained in moderate yields (10–25%) after purification by column chromatography.

The structures of oximes **5a**–**c** and cycloadducts **2a**–**c** were confirmed by their analytical and spectroscopic data (i.e., UV/Vis, FTIR, ^1H and ^{13}C NMR, and MALDI mass spectra). The matrix-assisted laser desorption time-of-flight (MALDI-TOF) spectra of **2a**–**c** exhibit the expected molecular ion peaks at m/z = 1258.9 (**2a**), 1297.4 (**2b**) and 1411.4 (**2c**), matching the calculated values. The ^1H NMR spectra of **2a**–**c** in $CDCl_3$ exhibit all expected signals with the correct integration ratios corresponding to the organic addend. ^{13}C NMR studies were only carried out on compound **2c** owing to the low solubility of compounds **2a** and **2b**. The ^{13}C NMR spectrum of compound **2c** is consistent with the proposed structure, exhibiting signals arising from the dendrimeric moiety as well as most of the signals of the fullerene system. The signals corresponding to the sp^3 carbon atoms of the C_{60} cage appear at δ = 83.6 and 80.0 ppm.

The model compounds **6** (PzC_{60}) and **7** (OxC_{60}) (Figure 2) were prepared according to a previously described procedure.[12b,15b]

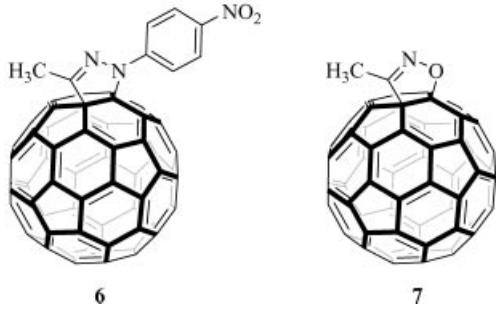

6 7

Figure 2. Reference compounds **6** and **7**.

Ab Initio B3LYP/3-21G Modeling

In order to gain an insight into the molecular and electronic structures, computational studies were performed using density functional methods (DFT) at the B3LYP/3-21G level of theory. The energy-minimized structures of compounds **1b** and **1c** are shown in Figure 3. For triads **1b** and **1c**, the two donor moieties are aligned in an L-shape with an angle of about 90° between the two donor units. The centre-to-centre distances (R_{CC}) between C_{60} and the donor entities were estimated to be about 13.3 and 15.0 Å for **1b** and **1c**, respectively. The electron density of the highest occupied molecular orbital (HOMO) was found to be located entirely on the two donor entities [$(R_2NPhV)_2Ph$ for

1b and $(ROPhV)_2Ph$ for **1c**], whereas the electron density of the lowest unoccupied molecular orbital (LUMO) was located on the C_{60} spheroid. These results also suggest the existence of charge-separated states: $[(FcV)_2Ph]^{\cdot+}$-$PzC_{60}^{\cdot-}$ for **1a**, $[(R_2NPhV)_2Ph]^{\cdot+}$-$PzC_{60}^{\cdot-}$ for **1b** and $[(ROPhV)_2Ph]^{\cdot+}$-$PzC_{60}^{\cdot-}$ for **1c**. It is also anticipated that the electronic coupling between the radical anion and radical cation of compound **1b** is not so large because of the completely separated HOMOs and LUMOs in Figure 3. Similar structures and MOs were obtained for analogous derivatives of $(Donor)_2Ph$-OxC_{60}.

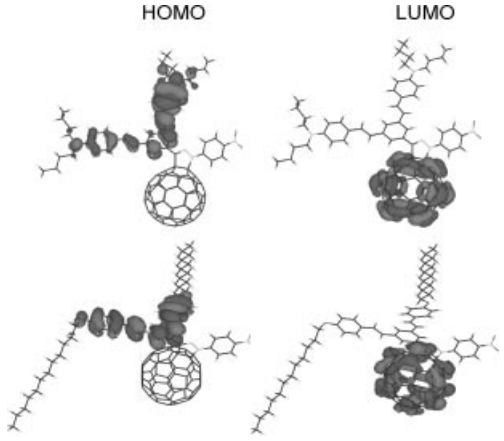

Figure 3. Optimized structures and the HOMO and LUMO of **1b** (upper) and **1c** (lower) calculated by ab initio B3LYP/3-21G methods.

Electrochemistry

The electrochemical properties of **1a**–**c** and **2a**–**c** were probed by cyclic (Figure 4) and Osteryoung voltammetry in an *o*-dichlorobenzene/acetonitrile solvent mixture (*o*-DCB/CH_3CN, 4:1 v/v) with nBu_4NClO_4 as the supporting electrolyte. The redox potentials measured versus Ag/Ag^+ at 100 mV s^{-1} are collected in Table 1.

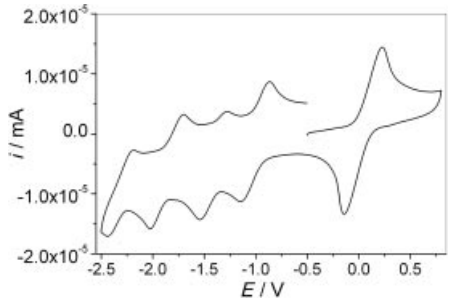

Figure 4. Cyclic voltammogram of compound **2a** in *o*-DCB/CH_3CN (4:1) (V versus $Ag/AgNO_3$; scan rate = 100 mV s^{-1}).

As a general feature, **1a**–**c** and **2a**–**c** gave rise to three reversible one-electron reduction waves in the cathodic observation window; these were attributed to the first three reduction potentials of the C_{60} cage. For **1a**–**c**, another irreversible reduction wave between the second and the third reduction potentials of the C_{60} cage (as a shoulder in the case of **1a**) was observed; this was assigned to the *p*-nitrophenyl group by comparison with related compounds.[15] Note that the first reduction potential of PzC_{60} derivatives **1a**–**c** exhibits an anodic shift (10–30 mV) relative to that of C_{60}, as observed previously for other Pz-based derivatives, as a result of the –I effect of the nitrogen atom linked directly to the C_{60} cage. On the other hand, the voltammograms of OxC_{60} derivatives **2a**–**c** exhibit a cathodic shift (20–40 mV) relative to the first reduction potential of C_{60}. This cathodic shift is lower (around 150 mV) than that observed in other C_{60} derivatives such as fulleropyrrolidines.

Table 1. Redox potentials for **1a**–**c**, **2a**–**c** and C_{60} determined by OSWV.[a]

	E_1^{red} [V]	E_2^{red} [V]	E_3^{red} [V]	E_4^{red} [V]	E_1^{ox} [V]
1a	–0.98	–1.40 (–1.66)[b]	–1.94	–2.25	–0.07
1b	–0.97	–1.35 (–1.70)[b]	–1.88	–2.24	0.48[b]
1c	–0.99	–1.38 (–1.74)[b]	–1.94	–2.36	–
2a	–1.02	–1.45	–1.94	–2.35	–0.09
2b	–1.04	–1.45	–1.93	–2.31	0.60[b]
2c	–1.04	–1.46	–1.92	–2.30	–
C_{60}	–1.00	–1.40	–1.87	–2.34	–

[a] Experimental conditions: V versus $Ag/AgNO_3$; glassy carbon as the working electrode; 0.1 M nBu_4NClO_4; scan rate: 100 mV s^{-1}; measured in *o*-DCB/CH_3CN (4:1 v/v) at room temperature. [b] Reversible, corresponding to the ferrocene addend, according to cyclic voltammetry.

In the anodic region, single reversible oxidation processes were observed for ferrocene (Fc) derivatives **1a** and **2a** at –0.07 and –0.09 V, respectively. A non-reversible oxidation was observed for *N*-butylaniline dyads at +0.48 V for **1b** and +0.60 V for **2b**; oxidation processes were not detected in the observation window for dodecyloxyphenyl derivatives **1c** and **2c**. Note that the experimentally determined HOMO–LUMO gap is as low as 0.91 eV for **1a** and 0.93 eV for **2a**. This value is of great interest as compounds with small HOMO–LUMO gaps are useful in optoelectronic de-

Table 2. Free-energy changes for charge separation ($-\Delta G_{CS}$) and charge recombination ($-\Delta G_{CR}$) in *o*-DCB/CH_3CN (4:1).[a]

	Solvent	$-\Delta G_{CR}$ [eV]	$-\Delta G_{CS}$ [eV] via $^1C_{60}$*
1a	PhCN	0.64	1.11
	toluene	1.53	0.22
1b	PhCN	1.22	0.53
	toluene	1.89	–0.14
2a	PhCN	0.67	1.08
	toluene	1.55	0.20
2b	PhCN	1.41	0.34
	toluene	2.09	–0.34

[a] $-\Delta G_{CR} = e[E_{ox}(D) - E_{red}(C_{60})] + \Delta G_S$; $-\Delta G_{CS} = \Delta E_{00} - (-\Delta G_{CR})$; ΔE_{00} = 1.75 eV for $^1C_{60}$*, $\Delta G_S = e^2/4\pi\varepsilon_o[(1/2R_+ + 1/2R_- - 1/R_{D-A})(1/\varepsilon_S) - (1/2R_+ + 1/2R_-)(1/\varepsilon_R)]$, where R_+ and R_- are the radii of the radical cation and radical anion, respectively, evaluated from MO calculations and ε_R and ε_S refer to solvent dielectric constants for electrochemical and photophysical measurements, respectively. The $-\Delta G_{CR}$ and $-\Delta G_{CS}$ values for **1c** and **2c** were not calculated as the first E_{ox} potentials were not observed.

vices.[21] Indeed a fullerene derivative with an electrochemical HOMO–LUMO gap, which is about 1 eV, was recently exploited as a molecular rectifier.[22]

From the first E_{red} of C_{60} and the first E_{ox} of the donor moieties, the free-energy changes (ΔG_{CR}) of the radical ion-pairs were calculated from the Weller equation[23] and are reported in Table 2. From ΔG_{CR} and the excited energies (E_{00}) of C_{60}, the free-energy changes of the charge-separation process (ΔG_{CS}) via the singlet excited state of C_{60} ($^1C_{60}$*) were calculated.[24] From these ΔG_{CS} values it can be deduced that the charge-separation process via the excited singlet state of C_{60} ($^1C_{60}$*) is sufficiently exothermic for **1a**,**b** and **2a**,**b** in PhCN. In toluene, the charge-separation process via $^1C_{60}$* is exothermic only in the case of **1a** and **2a**.

Steady-State Absorption Studies

The absorption spectra of the investigated compounds are shown in Figure 5. The absorption spectrum of **1a** exhibits an absorption band at 330 nm with a shoulder at 400 nm that is attributed to the PzC_{60} moiety, whereas the weak absorption in the 440–500 nm region is attributed to Fc units. The absorption spectrum of OxC_{60} **2a** exhibits only the peak at 330 nm in addition to the 440–500 nm band.

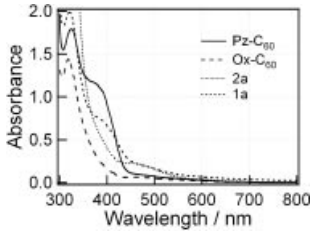

Figure 5. Steady-state absorption spectra of **1a** and **2a** along with the reference C_{60} compounds **6** (PzC_{60}) and **7** (OxC_{60}) in PhCN. The concentrations were maintained at 0.02 mM.

Similar spectral comparison was possible for the other derivatives, **1b**,**c** (330 nm band and 400 nm shoulder) and **2b**,**c** (330 nm band). Laser measurements were performed with 355 nm and 400 nm light which predominantly excited the PzC_{60} entity in the case of **1a**–**c** and the OxC_{60} entity in the case of **2a**–**c.**

Emission Studies

The fluorescence spectra of **1a**–**c** and **2a**–**c** along with the reference C_{60} compounds **6** (PzC_{60}) and **7** (OxC_{60}) in PhCN are shown in Figure 6. The measurements were carried out in different solvents by excitation with 400 nm light. In toluene and PhCN, the intensities of the emission band at 700 nm for **1a**–**c** and **2a**–**c** were significantly quenched relative to the C_{60} reference compounds. These observations suggest efficient quenching of the excited singlet state of the C_{60} ($^1C_{60}$*) moiety by the appended donor entities.

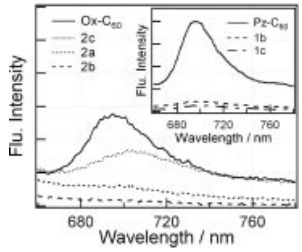

Figure 6. Steady-state fluorescence spectra of **2a**–**c** and reference compound **7** (OxC_{60}) in PhCN. Inset: fluorescence spectra of **1b**,**c** and the reference C_{60} compound **6** (PzC_{60}). The concentrations were maintained at 0.02 mM.

The time-resolved fluorescence spectrum obtained by applying 400 nm laser light in the time range 0–1 ns is shown in part a of Figure 7. The fluorescence peak position is in good agreement with those observed in the steady-state fluorescence measurements. The fluorescence time-profiles at 700 nm for **1a**–**c** and **2a**–**c** were recorded in PhCN and toluene (Figure 7, b). The fluorescence-time-profile of the reference compound **6** (PzC_{60}) exhibits a single exponential decay with a lifetime (τ_{f0}) of 1.3 ns, which matches well the reported value.[25] The fluorescence lifetimes (τ_f) of the studied compound moiety could be evaluated from curve-fitting of the fluorescence–time profile with two exponential components, as summarized in Table 3; single exponential fitting was possible in the cases of **1c**, **2b** and **2c** in toluene. The τ_f values in polar solvents are smaller than the τ_{f0} values, suggesting that the attachment of donor moieties introduces a new quenching pathway for the $^1C_{60}$* moiety. From the solvent dependence of the τ_f values, we infer charge-separation (CS) quenching of the $^1C_{60}$* moiety. The CS process via the $^1C_{60}$* moiety to the attached electron donors is

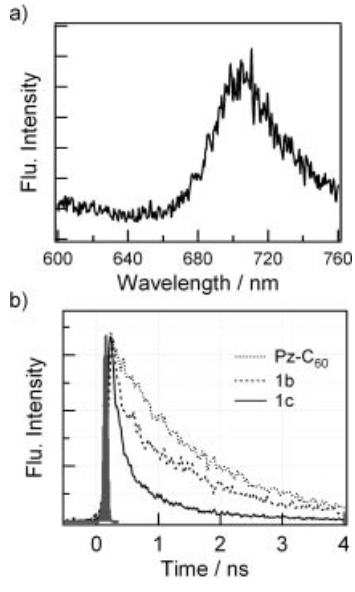

Figure 7. (a) Time-resolved fluorescence spectrum of **1b** in toluene and (b) time profiles of the fluorescence intensity for **1b** [$(R_2NPhV)_2$-Ph-PzC_{60}] and **1c** [$(ROPhV)_2$Ph-PzC_{60}] along with the reference compound **6** (PzC_{60}) in PhCN monitored at 700 nm; λ_{ex} = 400 nm.

supported by the energy levels of the CS states of **1a**–**c** being lower than that of $^1C_{60}$* as well as by the transient absorption bands in the near-IR region that can be assigned to $C_{60}^{\cdot-}$, as described in the forthcoming section.

Table 3. Fluorescence lifetimes (τ_f), rate constants (k_{CS}) and quantum yields (Φ_{CS}) for CS via the $^1C_{60}$* moieties of **1a**–**c** and **2a**–**c**.

	Solvent	τ_f [ps] (fraction [%])	k_{CS}[a] [10^9 s^{-1}]	Φ_{CS}[a]
1a	PhCN	<20	>10	>0.98
	o-DCB	92 (52) 1200 (48)	10	0.97
	toluene	170 (70) 1300 (30)	5.5	0.93
1b	PhCN	130 (52) 1500 (48)	7.1	0.90
	toluene	1300 (100)	–[b]	–[b]
1c	PhCN	200 (80)1200 (20)	4.2	0.84
	toluene	1500 (100)	–[b]	–[b]
2a	PhCN	<20	>10	>0.98
	toluene	200 (60) 1400 (10)	4.6	0.92
2b	PhCN	166 (66) 1300 (34)	5.5	0.88
	toluene	1400 (100)	–[b]	–[b]
2c	PhCN	500 (57) 1600 (43)	1.3	0.64
	toluene	1500 (100)	–[b]	–[b]

[a] These values were calculated from the fast decay; $k_{CS} = (1/\tau_f) - (1/\tau_{f0})$ and $\Phi_{CS} = k_{CS}/(1/\tau_f)$. [b] No charge separation.

The rate constants (k_{CS}) and quantum yields (Φ_{CS}) for CS via the $^1C_{60}$* moieties were evaluated based on τ_0 and short τ_f values, as listed in Table 3. The slow fluorescence lifetimes can be considered as delayed fluorescence resulting from a thermal equilibrium with the CS state because the fraction of the slowly decaying component increases with the instability of the CS state. Both k_{CS} and Φ_{CS} values for **1a** and **1b** in PhCN were found to be higher than those for **1c**, indicating the lower donor ability of the 4-dodecyloxyphenyl units in comparison with ferrocene and dibutylaniline units. For compound **1a**, the k_{CS} values in polar solvents are larger than in toluene.

Nanosecond Transient Absorption Spectra

Nanosecond transient absorption spectroscopy in the visible and near-IR regions was performed to confirm the existence of the CS state and to monitor the charge-recombination (CR) processes of **1a**–**c** and **2a**–**c** in PhCN, *o*-DCB and toluene. The transient absorption spectra of **1a** in toluene are shown in Figure 8 (a); the absorption peak at 700 nm, attributed to the $^3C_{60}$* moiety, undergoes slow decay, whereas the broad absorption band in the range 1000–1500 nm can be attributed to the pyrazolo-C_{60} radical anion ($PzC_{60}^{\cdot-}$). The transient absorption bands of the donor moiety [$(FcV)_2Ph^{\cdot+}$] may be hidden by these huge broad bands because a weak absorption is expected from the Fc^+ moiety. The time profiles of the absorption peaks are shown in the insets of Figure 8 (a); the immediate rise of the 1500 nm band after a 6 ns laser light pulse supports a very quick CS process, probably corresponding to the fluorescence decay. After reaching a maximum, the time profile begins to decay; the 1520 nm band decayed in toluene with a CR rate constant (k_{CR}) of 6.4×10^6 s^{-1} for the radical-ion pair [$(FcV)_2Ph]^{\cdot+}$-$PzC_{60}^{\cdot-}$, which gives a lifetime for the radical-ion pair (τ_{RIP}) of 160 ns (as listed in Table 4). This τ_{RIP} value is greater than that of the monoferrocene-PzC_{60} radical-ion pair (35 ns in toluene).[26] This observation clearly indicates communication between the two Fc moieties through the vinylenephenylene π bonds causing hole migration between the two ferrocene moieties, prolonging the lifetime of the radical ion-pair of **1a** compared with monoferrocene-PzC_{60}. Similarly, the transient absorption spectra of **1a** in PhCN (Figure 8, b) and *o*-DCB exhibit the same characteristic peaks as in toluene. The k_{CR} values for the radical-ion pair were evaluated as 9.2×10^6 (PhCN) and 6.7×10^6 s^{-1} (*o*-DCB), which equate to lifetimes of the radical-ion pair (τ_{RIP}) of 110 (PhCN) and 149 ns (*o*-DCB). The τ_{RIP} in PhCN is shorter than that in toluene and *o*-DCB suggesting that the CR process belongs to the inverted region of the Marcus parabola as the reorganization energy may be smaller than the absolute value of the free energy of the CR process (ΔG_{CR}) even in PhCN.[27,28]

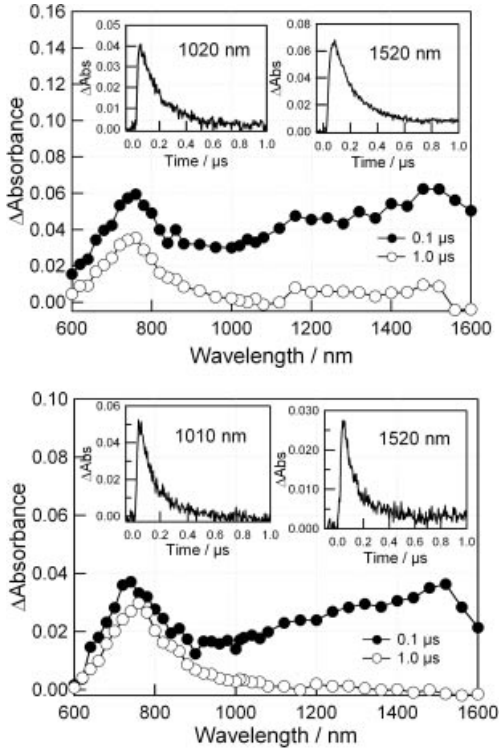

Figure 8. Transient absorption spectra obtained by 355 nm laser light photolysis of **1a** in Ar-saturated (a) toluene and (b) PhCN; concentrations kept at 0.08 mM.

The transient absorption spectrum of **2a** in PhCN exhibited only a weak absorption peak at 700 nm with slow decay of the $^3C_{60}$* moiety, without observing the bands of the radical ion-pair. Thus, a CR process faster than the nanosecond laser light pulse (ca. 6 ns) was suggested. This indicates that the isoxazoline ring connecting the Fc and C_{60} moieties does not stabilize the charge-separated state [$(FcV)_2$-$Ph]^{\cdot+}$-$OxC_{60}^{\cdot-}$. The pyrazoline ring in **1a** has a stabilizing effect on the radical-ion pair [$(FcV)_2Ph]^{\cdot+}$-$PzC_{60}^{\cdot-}$.

Table 4. Rate constants (k_{CR}) for CR and lifetimes of the radical-ion pairs (τ_{RIP}) of **1a–c** and **2a–c**.

	Solvent	k_{CR} [s^{-1}]	τ_{RIP} [ns]
1a	PhCN	9.2×10^6	110
	o-DCB	6.7×10^6	149
	toluene	6.4×10^6	160
1b	PhCN	1.1×10^7	90
	toluene	_[a]	_[a]
1c	PhCN	1.5×10^8	<7
	toluene	_[a]	_[a]
2a	PhCN	$>5\times10^8$	<2
	toluene	$>5\times10^8$	<2
2b	PhCN	4.1×10^7	25
	toluene	_[a]	_[a]
2c	PhCN	$>5\times10^8$	<2
	toluene	_[a]	_[a]

[a] No charge separation.

In the case of **1b** the transient absorption spectra in PhCN (Figure 9, a) exhibit an absorption peak at 700 nm that is assigned to the $^3C_{60}$* moiety. At 1000 nm, only a weak transient absorption remained as a trace of the CS state $[(R_2NPhV)_2Ph]^{\cdot+}$-$PzC_{60}^{\cdot-}$. This low yield of $[(R_2NPhV)_2Ph]^{\cdot+}$-$PzC_{60}^{\cdot-}$ may be related to the high fraction of the slow fluorescence decay (Table 3) which causes a higher yield of the triplet state of C_{60}. In toluene, the transient absorption spectrum of **1b** exhibits the absorption peak of the $^3C_{60}$* moiety with slow decay suggesting no CS process, in agreement with a non-quenched fluorescence lifetime.

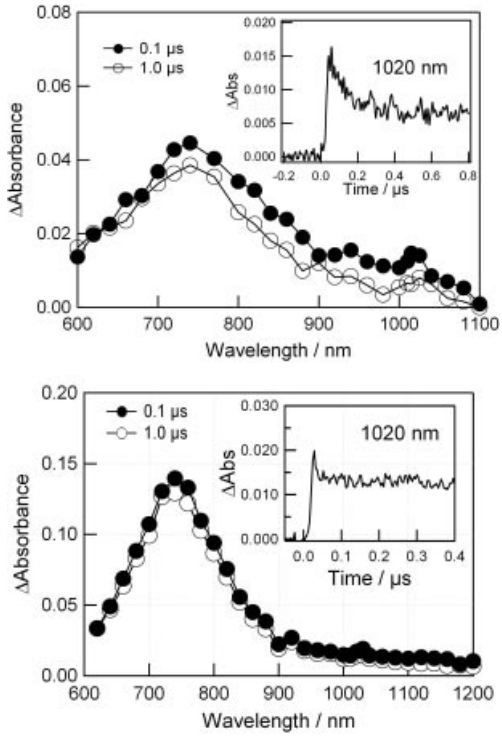

Figure 9. Transient absorption spectra obtained by 355 nm laser light photolysis of (a) **1b** and (b) **1c** (0.08 mM) in Ar-saturated PhCN.

The transient absorption spectra of **1c** in PhCN are shown in Figure 9 (b) and the absorption peak at 700 nm was attributed to the $^3C_{60}$* moiety with slow decay. A weak transient absorption appeared at 1020 nm with rapid decay, suggesting the short-lived $C_{60}^{\cdot-}$ moiety. The τ_{RIP} value was evaluated to be <7 ns, which is significantly smaller than those for **1a** and **1b** in PhCN. Compared with the amino group, the ether group has a lower donor ability; thus the factor that stabilizes $[(ROPhV)_2Ph]^{\cdot+}$-$PzC_{60}^{\cdot-}$ is no longer present.

The energy level diagram for compounds **1a–c** in PhCN and toluene is shown in Figure 10. For **1a**, the exothermic CS process can be well understood in terms of this energy diagram. The reason for the higher k_{CS} in PhCN than in toluene can be easily understood when the reorganization energy is close to 1.0 eV as the ΔG_{CS} value suggests the top region of the Marcus parabola in PhCN. For the CR process, the solvent effect on $[(FcV)_2Ph]^{\cdot+}$-$PzC_{60}^{\cdot-}$ can be explained by the Marcus parabola. For **1b**,**c**, the CS process does not take place in toluene because in this solvent it is a highly endothermic process. The phenomena observed for **2a–c** can be qualitatively explained using a similar energy diagram.

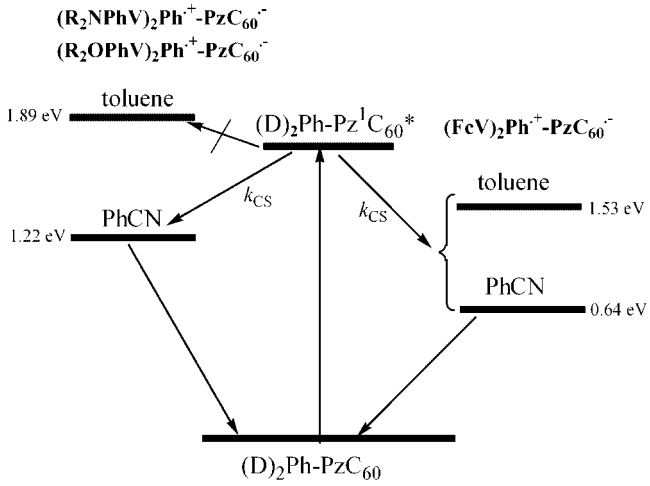

Figure 10. Energy level diagram for **1a–c** in PhCN and toluene.

Intermolecular Electron Transfer between C_{60} and the Donor Moieties

The photoexcitation of pristine C_{60} (0.08 mM) in the presence of electron donors **4a–c** and **5a** in argon-saturated PhCN using a 532 nm laser (Figure 11) leads to an acceleration of the decay of the C_{60} triplet state at 760 nm. With the decay of $^3C_{60}$*, the concomitant rise of $C_{60}^{\cdot-}$ at 1100 nm was observed, as shown in the time profiles in the inset in Figure 11. The decay of $^3C_{60}$* and the rise of $C_{60}^{\cdot-}$ seem to be mirror images. These observations indicate that the intermolecular electron transfer takes place via $^3C_{60}$*.

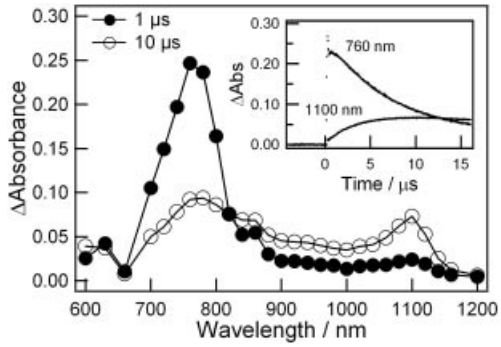

Figure 11. Transient spectra obtained by 532 nm laser light excitation of C_{60} (0.08 mM) in the presence of compound **4b** (0.1 mM) in Ar-saturated PhCN.

Furthermore, the contribution of $^3C_{60}$* to the electron-transfer process was confirmed by an O_2 effect on the decreasing yields of $C_{60}^{\bullet-}$. The decay of $^3C_{60}$* was accelerated by addition of O_2 in the absence of electron donors indicating that $^3C_{60}$* was quenched by energy transfer to O_2 (the rate constant is denoted as k_{O2}) to yield singlet oxygen ($^1O_2$); k_{O2} was evaluated as 2×10^{10} M^{-1} s^{-1} (assuming $[O_2]$ = 0.2 mM) in PhCN.[29]

The rate constants for the bimolecular quenching (k_q^T) of $^3C_{60}$* with electron donors **4a**–**c** and **5a** were evaluated under the pseudo-first-order condition [$^3C_{60}$*] << [electron donors] and are given in Table 5. The quantum yield for the intermolecular electron-transfer process (Φ_{et}^T) can be calculated from the ratio of the maximal concentration of the generated $C_{60}^{\bullet-}$ to the initial concentration of $^3C_{60}$*. The Φ_{et}^T values decrease in the order HzNBu (**4b**) >> HzFc (**4a**) ≈ OxFc (**5a**) > HzOdod (**4c**); the small Φ_{et} values for the ferrocene derivatives can be attributed to energy transfer from $^3C_{60}$*.[30] The electron-transfer rate constants (k_{et}) were finally obtained from the equation $k_{et} = k_q\Phi_{et}$. k_{et}^T values were evaluated to be of the order of 10^8 M^{-1} s^{-1} for HzNBu (**4b**), HzFc (**4a**) and OxFc (**5a**) and of the order of 10^7 M^{-1} s^{-1} for HzOdod (**4c**), all of which are considerably smaller than the diffusion-controlled limit (k_{diff} = 5.6×10^9 M^{-1} s^{-1}) in PhCN.[29] The higher rates and efficiencies for electron transfer of **4a** and **4b** compared with **4c** may be explained by the higher donor ability of ferrocene and dibutylaniline moieties compared with the dodecyloxyphenyl moiety, as estimated from the oxidation potentials in Table 1.

Table 5. Rate constants (k_q) for quenching of $^3C_{60}$*, quantum yields (Φ_{et}), rate constants (k_{et}) for electron transfer via $^3C_{60}$* with different donors in PhCN and rate constants for the back electron transfer (k_{bet}).

Electron donor	k_q [10^9 M^{-1} s^{-1}]	Φ_{et}	k_{et} [10^8 M^{-1} s^{-1}]	k_{bet} [10^9 M^{-1} s^{-1}]
OxFc (**5a**)	4.4	0.10	4.2	8.8
HzFc (**4a**)	1.9	0.10	1.9	9.2
HzNBu (**4b**)	1.6	0.37	5.9	6.3
HzOdod (**4c**)	0.47	0.07	0.33	4.1

From the time profile of $C_{60}^{\bullet-}$ over a prolonged period after the laser pulse in an argon-saturated PhCN solution, it is clear that $C_{60}^{\bullet-}$ begins to decay slowly after reaching the maximal absorbance. The decay time profile was curve-fitted with second-order kinetics, suggesting that a bimolecular back-electron-transfer process takes place after $C_{60}^{\bullet-}$ and the radical cations of the donors are solvated as the free radical ions. The k_{bet} values were evaluated to be of the order of 10^9 M^{-1} s^{-1}, as listed in Table 5; these values are near the diffusion-controlled limit in PhCN. These observations suggest that the forward and backward electron-transfer processes occur reversibly.

Conclusions

The synthesis of new pyrazolo- and isoxazolo[60]fullerenes with covalently attached phenylenevinylene systems with two ferrocene, dibutylaniline or dodecyloxyphenyl groups as donors in the periphery has been accomplished. Fast charge separation via the excited singlet state of C_{60} and relatively slow charge recombination were confirmed by photophysical techniques. First, the dual-donor systems are better than the monodonor systems in obtaining prolonged charge-separation states with the trends as reported for the multidonor systems.[9,10] The second point revealed in the present study is the effect of the bridges (pyrazoline and isoxazoline rings) used to connect the donors to the fullerene moieties; the pyrazoline ring acts as a better bridge than isoxazoline in the sense of high charge-separation efficiencies and slow charge-recombination rates.

Experimental Section

General Remarks: All cycloaddition reactions were performed under argon. C_{60} was purchased from MER Corporation (Tucson, AZ). TLC using Merck silica gel 60-F_{254} was employed to monitor the cycloaddition reactions. Microwave irradiation was performed using a Microwave Synthesis workstation (CEM). ^{1}H and ^{13}C NMR spectra were recorded with Varian Mercury 200 and Inova 500 spectrometers. FTIR spectra were recorded with a Nicolet Impact 410 spectrometer using KBr disks. MALDI-TOF mass spectra were obtained with a Bruker ReflexIII spectrometer. Elemental analyses were performed with a Perkin-Elmer 2400 CHNS/O Series II elemental analyzer.

The UV/Vis spectral measurements were carried out with a Jasco model V570 DS and a Shimadzu spectrophotometer. Steady-state fluorescence spectra were measured with a Shimadzu RF-5300 PC spectrofluorophotometer equipped with a photomultiplier tube having high sensitivity in the 700–800 nm region. Cyclic voltammetry measurements were carried out with an Autolab PGSTAT 30 potentiostat using a BAS MF-2062 Ag/0.01 M $AgNO_3$, 0.1 M (n-$C_4H_9)_4NClO_4$ in CH_3CN reference electrode, an auxiliary electrode consisting of a Pt wire and a Metrohm 6.1247.000 conventional glassy carbon electrode (3 mm o.d.) as a working electrode directly immersed in the o-DCB/CH_3CN (4:1) solution. A 10 mL electrochemical cell from BAS, Model VC-2, was also used. The reference potential was shifted by 290 mV towards a more negative potential compared with the Ag/AgCl scale. $E_{1/2}$ values were taken as the

average of the anodic and cathodic peak potentials. A scan rate of 100 mV s^{-1} was used.

Picosecond time-resolved fluorescence spectra were measured using a single-photon counting method with second harmonic generation (SHG, 400 nm) from a Ti:sapphire laser (Spectra-Physica, Tsunami 3950-L2S, 1.5 ps fwhm) and a streakscope (Hamamatsu Photonics) equipped with a polychromator as excitation source and detector, respectively. The nanosecond transient absorption measurements in the near-IR region were measured by laser-flash photolysis; 355 nm light from a Nd:YAG laser with OPA (Spectra-Physics and Quanta-Ray GCR-130, 6 ns fwhm) was used as the excitation source. For transient absorption spectra in the near-IR region (600–1200 nm), monitoring light from a pulsed Xe lamp was detected with a germanium avalanche-photodiode module (Hamamatsu Photonics). All the samples were deaerated in a quartz cell (1 × 1 cm) by bubbling Ar through the solution for 15 min.

Molecular Orbital Calculations: The computational calculations were performed by ab initio B3LYP/3-21G methods using the GAUSSIAN 03[31] software package on high speed computers.

General Procedure for the Synthesis of the Hydrazones 4a–c: The syntheses were carried out according to the general method described in the literature from the corresponding aldehydes.[19] A solution of an aldehyde **3a**–**c**[18] (0.06 mmol), 4-nitrophenylhydrazine (0.06 mmol) and two drops of AcOH in EtOH (10 mL) was refluxed for 2 h. The solution was cooled to room temperature and then kept at 0 °C for 12 h. The solid was filtered off and the crude product purified by recrystallization from EtOH.

(*E*,*E*)-3,5-Bis(ferrocenylvinyl)benzaldehyde 4-Nitrophenylhydrazone (4a): Yield: 65% (25 mg); m.p. 230 °C (decomp.). FTIR (KBr): $\tilde{\nu}$ = 2924, 2854, 1750, 1596, 1321 cm^{-1}. ^{1}H NMR ($CDCl_3$): δ = 4.17 (s, 10 H), 4.32 (t, J = 1.6 Hz, 4 H), 4.52 (t, J = 1.4 Hz, 4 H), 6.75 (d, J = 16.0 Hz, 2 H), 7.00 (d, J = 16.0 Hz, 2 H), 7.20 (d, J = 9.0 Hz, 2 H), 7.52 (s, 1 H), 7.58 (s, 2 H), 7.83 (s, 1 H), 8.08 (br. s, 1 H), 8.24 (d, J = 9.0 Hz, 2 H) ppm. ^{13}C NMR ($CDCl_3$): δ = 149.6, 141.6, 139.0, 135.0, 128.4, 126.5, 125.5, 124.3, 122.8, 112.1, 83.2, 69.5, 67.2 ppm. UV/Vis (CH_2Cl_2): λ_{max} (logε) = 317.0 (4.4), 397.0 nm (4.4). MS (MALDI-TOF): m/z = 661.2 [M]$^+$.

(*E*,*E*)-3,5-Bis[4-(dibutylamino)styryl]benzaldehyde 4-Nitrophenylhydrazone (4b): Yield: 82% (35 mg); m.p. 113–115 °C. FTIR (KBr): $\tilde{\nu}$ = 2259, 1563, 1215 cm^{-1}. ^{1}H NMR ($CDCl_3$): δ = 0.97 (t, J = 7.2 Hz, 12 H), 1.23–1.41 (m, 8 H), 1.54–1.64 (m, 8 H), 3.30 (t, J = 7.5 Hz, 8 H), 6.64 (d, J = 9.0 Hz, 4 H), 6.89 (d, J = 16.5 Hz, 2 H), 7.10 (d, J = 16.5 Hz, 2 H), 7.10 (d, J = 9.3 Hz, 2 H), 7.41 (d, J = 9.0 Hz, 4 H), 7.53 (s, 2 H), 7.54 (s, 1 H), 7.71 (s, 1 H), 8.02 (br. s, 1 H), 8.18 (d, J = 9.3 Hz, 2 H) ppm. ^{13}C NMR ($CDCl_3$): δ = 149.5, 148.2, 141.9, 140.5, 139.2, 134.6, 129.8, 127.9, 126.1, 124.7, 124.4, 123.1, 122.6, 111.8, 50.8, 29.7, 20.4, 14.0 ppm. UV/Vis (CH_2Cl_2): λ_{max} (logε) = 337.0 (4.1), 387.0 nm (4.3). MS (MALDI-TOF): m/z = 699.694 [M]$^+$.

(*E*,*E*)-3,5-Bis(4-dodecyloxystyryl)benzaldehyde 4-Nitrophenylhydrazone (4c):[10] Yield: 90% (45 mg); m.p. 115–117 °C. FTIR (KBr): $\tilde{\nu}$ = 3278, 2850, 1592, 1512, 1464, 1323, 1250, 1176, 1109, 834 cm^{-1}. ^{1}H NMR ($CDCl_3$): δ = 0.89 (t, J = 6.9 Hz, 6 H), 1.28 (br. s, 36 H), 1.77–1.84 (m, 4 H), 3.99 (t, J = 6.5 Hz, 4 H), 6.92 (d, J = 8.7 Hz, 4 H), 7.09 (br. s, 4 H), 7.17 (d, J = 9.1 Hz, 2 H), 7.49 (d, J = 8.7 Hz, 4 H), 7.62 (s, 2 H), 7.64 (s, 2 H), 7.80 (s, 1 H), 8.07 (br. s, 1 H), 8.22 (d, J = 9.1 Hz, 2 H) ppm. ^{13}C NMR ($CDCl_3$): δ = 159.3, 149.5, 141.5, 140.6, 138.8, 134.9, 129.7, 129.5, 128.1, 126.4, 125.8, 125.3, 123.5, 114.9, 112.0, 68.3, 32.1, 29.9, 29.8, 29.6, 29.5, 26.2, 22.9, 14.3 ppm. UV/Vis (CH_2Cl_2): λ_{max} (logε) = 331.0 (4.8), 397.0 nm (4.6). MS (MALDI-TOF): m/z = 813.4.

General Procedure for the Synthesis of Oximes 5a–c: The syntheses were carried out according to the general method described in the literature from the corresponding aldehydes **3a**–**c**.[16] A solution of an aldehyde **3a**–**c**[18] (0.6 mmol), hydroxylamine hydrochloride (4.8 mmol) and anhydrous pyridine (15 μL) in EtOH/CH_2Cl_2 (10 mL/3 mL) as solvent was refluxed for 2 h. The solvent was removed under reduced pressure, the solid was treated with water (5 mL) and the solution cooled in an ice bath. The resulting precipitate was filtered off and purified by recrystallization from EtOH.

(*E*,*E*)-3,5-Bis(ferrocenylvinyl)benzaldoxime (5a): Yield: 89% (287 mg); m.p. 131–133 °C (d). FTIR (KBr): $\tilde{\nu}$ = 1686, 1604, 1368, 1189, 963 cm^{-1}. ^{1}H NMR ($CDCl_3$): δ = 4.16 (s, 10 H), 4.31 (t, J = 1.6 Hz, 4 H), 4.49 (t, J = 1.5 Hz, 4 H), 6.72 (d, J = 15.8 Hz, 2 H), 6.97 (d, J = 16.2 Hz, 2 H), 7.48 (s, 1 H), 7.51 (s, 2 H), 7.66 (br. s, 1 H), 8.19 (s, 1 H) ppm. ^{13}C NMR ($CDCl_3$): δ = 150.5, 138.7, 132.6, 128.1, 125.1, 124.9, 122.4, 82.9, 69.2, 66.9 ppm. UV/Vis (CH_2Cl_2): λ_{max} (logε) = 316.0 nm (4.4). MS (MALDI-TOF): m/z = 540.478 [M]$^+$.

(*E*,*E*)-3,5-Bis[4-(dibutylamino)styryl]benzaldoxime (5b): Yield: 99% (342 mg). FTIR (KBr): $\tilde{\nu}$ = 2362, 1631, 1582, 982 cm^{-1}. ^{1}H NMR ($CDCl_3$): δ = 0.98 (t, J = 7.4 Hz, 12 H), 1.15–1.48 (m, 8 H), 1.49–1.79 (m, 8 H), 3.31 (t, J = 7.4 Hz, 8 H), 6.65 (d, J = 8.4 Hz, 4 H), 6.89 (d, J = 16.2 Hz, 2 H), 7.11 (d, J = 16.2 Hz, 2 H), 7.41 (d, J = 8.2 Hz, 4 H), 7.52 (s, 2 H), 7.57 (s, 1 H), 8.18 (s, 1 H) ppm. ^{13}C NMR ($CDCl_3$): δ = 160.7, 148.2, 132.6, 130.3, 129.5, 129.0, 128.0, 127.4, 124.4, 122.7, 111.6, 50.7, 29.3, 20.3, 14.0 ppm. UV/Vis (CH_2Cl_2): λ_{max} (logε) = 374 nm (4.5). MS (MALDI-TOF): m/z = 579.252 [M]$^+$.

(*E*,*E*)-3,5-Bis(4-dodecyloxystyryl)benzaldoxime (5c): Yield: 99% (409.5 mg); m.p. 103–104 °C. FTIR (KBr): $\tilde{\nu}$ = 1607, 1587 cm^{-1}. ^{1}H NMR ($CDCl_3$): δ = 0.91 (t, J = 6.6 Hz, 6 H), 1.16–1.60 (m, 36 H), 1.81 (dt, J = 8.4 Hz, J = 6.5 Hz, 4 H), 3.99 (t, J = 6.5 Hz, 4 H), 6.90 (d, J = 8.4 Hz, 4 H), 6.97 (d, J = 16.2 Hz, 2 H), 7.14 (d, J = 16.0 Hz, 2 H), 7.46 (d, J = 8.7 Hz, 4 H), 7.57 (s, 2 H), 7.68 (s, 1 H), 7.75 (br. s, 1 H), 8.19 (s, 1 H) ppm. ^{13}C NMR ($CDCl_3$): δ = 158.0, 152.0, 134.9, 131.0, 126.5, 126.8, 126.2, 125.9, 124.8, 114.1, 72.3, 32.5, 30.6, 30.4, 30.3, 30.3, 30.0, 26.6, 23.1, 14.0 ppm. UV/Vis (CH_2Cl_2): λ_{max} (logε) = 332.0 nm (4.9). MS (MALDI-TOF): m/z = 693.5821 [M]$^+$.

General Procedure for the Synthesis of Pyrazolo[60]fullerenes 1a–c: Dry pyridine (5 μL) was added to a solution of the corresponding hydrazone **4a**–**c** (0.05 mmol) in $CHCl_3$ (10 mL). The solution was cooled to 0 °C and *N*-chlorosuccinimide (0.12 mmol) was added. The mixture was stirred for 30 min at 0 °C and 1 h at room temperature. A solution of C_{60} (0.06 mmol) and Et_3N (0.15 mmol) in toluene (45 mL) was added to the solid. The mixture was then treated according to the process described for each compound. After the corresponding reaction time, the solvent was removed under reduced pressure. The resulting solid was purified by silica gel flash chromatography using toluene/hexane as eluent. Repetitive centrifugation with methanol and diethyl ether was performed to further purify the solid.

Compound 1a: The solution was stirred at room temperature for 90 min. The resulting solid was purified by silica gel flash chromatography using toluene/hexane (8:2) as eluent. Yield: 19% (14 mg). FTIR (KBr): $\tilde{\nu}$ = 3412, 2221, 1594, 1257, 525 cm^{-1}. ^{1}H NMR ($CDCl_3$): δ = 4.14 (s, 10 H), 4.32 (t, J = 1.6 Hz, 4 H), 4.48 (t, J = 1.5 Hz, 4 H), 6.70 (d, J = 16.4 Hz, 2 H), 6.89 (d, J = 16.4 Hz, 2 H), 7.51 (s, 1 H), 8.11 (s, 2 H), 8.32 (d, J = 9.4 Hz, 2 H), 8.36 (d, J = 9.2 Hz, 2 H) ppm. ^{13}C NMR ($CDCl_3$): δ = 153.8, 146.5, 145.7, 144.3, 143.4, 143.0, 142.8, 141.7, 140.6, 139.6, 136.7, 132.3, 129.9, 129.1, 127.3, 125.7, 125.4, 125.0, 122.5, 119.7, 89.2, 73.0, 70.0, 69.4,

67.6, 64.01 ppm. UV/Vis (CH_2Cl_2): λ_{max} ($\log\varepsilon$) = 327.0 (3.8), 430.0 nm (2.9). MS (MALDI-TOF): *m/z* = 1379.1 $[M]^+$, 719.9 $[C_{60}]^+$.

Compound 1b: The solution was stirred at room temperature for 90 min. The resulting solid was purified by silica gel flash chromatography using toluene/hexane (7:3) as eluent. Yield: 15% (11 mg). FTIR (KBr): $\tilde{\nu}$ = 3372, 1605, 1261, 741, 526 cm^{-1}. ^1H NMR ($CDCl_3$): δ = 0.96 (t, *J* = 7.4 Hz, 12 H), 1.19–1.45 (m, 8 H), 1.50–1.70 (m, 8 H), 3.30 (t, *J* = 7.2 Hz, 8 H), 6.63 (d, *J* = 8.8 Hz, 4 H), 6.92 (d, *J* = 16.8 Hz, 2 H), 7.07 (d, *J* = 16.2 Hz, 2 H), 7.37 (d, *J* = 8.8 Hz, 4 H), 7.66 (s, 1 H), 8.13 (s, 2 H), 8.30 (d, *J* = 9.8 Hz, 2 H), 8.37 (d, *J* = 9.4 Hz, 2 H) ppm. ^{13}C NMR ($CDCl_3$): δ = 149.5, 148.2, 141.9, 140.5, 139.2, 134.6, 129.8, 127.9, 126.1, 124.7, 124.4, 123.1, 122.6, 111.8, 50.8, 29.7, 20.4, 14 ppm. UV/Vis (CH_2Cl_2): λ_{max} ($\log\varepsilon$) = 326.0 (4.1), 389.0 (3.9), 501.0 nm (2.9). MS (MALDI-TOF): *m/z* = 1417.4 $[M]^+$, 720.0 $[C_{60}]^+$.

Compound 1c: The mixture was irradiated in a focused microwave reactor at 210 W for 20 min. The resulting solid was purified by silica gel flash chromatography using toluene/hexane (1:1) as eluent. Yield: 31% (24 mg). FTIR (KBr): $\tilde{\nu}$ = 2846, 1580, 1507, 1454, 1321, 1169, 1109, 525 cm^{-1}. ^1H NMR ($CDCl_3$): δ = 0.89 (t, *J* = 6.5 Hz, 6 H), 1.27 (br. s, 36 H), 1.76–1.83 (m, 4 H), 3.98 (t, *J* = 6.5 Hz, 4 H), 6.90 (d, *J* = 8.4 Hz, 4 H), 7.03 (d, *J* = 16.5 Hz, 2 H), 7.12 (d, *J* = 16.5 Hz, 2 H), 7.45 (d, *J* = 8.4 Hz, 4 H), 7.71 (s, 1 H), 8.20 (s, 2 H), 8.29 (d, *J* = 9.5 Hz, 2 H), 8.36 (d, *J* = 9.8 Hz, 2 H) ppm. ^{13}C NMR ($CDCl_3$): δ = 159.4, 149.9, 147.8, 147.4, 147.1, 146.6, 146.5, 146.3, 146.1, 145.8, 145.6, 145.5, 144.7, 144.6, 144.3, 143.4, 143.2, 142.7, 142.5, 142.3, 142.2, 140.6, 139.6, 139.0, 137.3, 136.4, 132.2, 130.0, 129.5, 128.1, 125.6, 119.6, 114.9, 68.3, 32.1, 29.8, 29.6, 29.5, 29.4, 26.2, 22.9, 14.3 ppm. UV/Vis (CH_2Cl_2): λ_{max} ($\log\varepsilon$) = 254.0 (5.1), 326.0 nm (5.0). MS (MALDI-TOF): *m/z* = 1531.2 $[M]^+$, 720.0 $[C_{60}]^+$.

General Procedure for the Synthesis of Isoxazolo[60]fullerenes 2a–c: This procedure is a modification of the general method for the cycloaddition of nitrile oxides to olefins.[32] Dry pyridine (5 μL was added to a solution of the appropriate aldoxime (0.06 mmol) in dry chloroform (10 mL). The mixture was cooled to 0 °C and *N*-chlorosuccinimide (0.12 mmol) was added to the solution and the mixture was stirred for 60 min. A solution of C_{60} (0.06 mmol) in dry toluene (45 mL) was added. The mixture was treated with triethylamine (0.15 mmol). The mixture was then treated according to the process described for each compound. After the corresponding reaction time, the solvent was removed under reduced pressure. The resulting solid was purified by silica gel flash chromatography using toluene/hexane as eluent. Repetitive centrifugation with methanol and diethyl ether was performed to further purify the solid.

Compound 2a: The solution was stirred at 0 °C for 2 h. The resulting solid was purified by silica gel flash chromatography using toluene/hexane (6:4) as eluent. Yield: 25% (19 mg). FTIR (KBr): $\tilde{\nu}$ = 1659, 1498, 1465, 525 cm^{-1}. ^1H NMR ($CDCl_3$): δ = 4.14 (s, 10 H), 4.32 (t, *J* = 1.6 Hz, 4 H), 4.48 (t, *J* = 1.5 Hz, 4 H), 6.73 (d, *J* = 16.3 Hz, 2 H), 6.94 (d, *J* = 16.3 Hz, 2 H), 7.54 (s, 1 H), 8.17 (s, 2 H) ppm. UV/Vis (CH_2Cl_2): λ_{max} ($\log\varepsilon$) = 327.0 (3.8), 430.0 nm (2.9). MS (MALDI-TOF): *m/z* = 1258.9 $[M]^+$, 720 $[C_{60}]^+$.

Compound 2b: The solution was stirred at room temperature for 2.5 h. The resulting solid was purified by silica gel flash chromatography using toluene/hexane (8:2) as eluent. Yield: 10% (8 mg). FTIR (KBr): $\tilde{\nu}$ = 1713, 1448, 526 cm^{-1}. ^1H NMR ($CDCl_3$): δ = 0.96 (t, *J* = 7.4 Hz, 12 H), 1.18–1.41 (m, 8 H), 1.45–1.78 (m, 8 H), 3.29 (t, *J* = 7.4 Hz, 8 H), 6.62 (d, *J* = 8.4 Hz, 4 H), 6.90 (d, *J* = 16.0 Hz, 2 H), 7.07 (d, *J* = 16.2 Hz, 2 H), 7.37 (d, *J* = 8.6 Hz, 4 H), 7.66 (s, 1 H), 8.11 (s, 2 H) ppm. UV/Vis (CH_2Cl_2): λ_{max} ($\log\varepsilon$) = 323.0 (4.5), 429.0 nm (3.5). MS (MALDI-TOF): *m/z* = 1297.4 $[M]^+$, 720 $[C_{60}]^+$.

Compound 2c: The solution was irradiated with microwaves for 40 min at 210 W of power. The resulting solid was purified by silica gel flash chromatography using toluene/hexane (8:2) as eluent. Yield: 21% (18 mg). FTIR (KBr): $\tilde{\nu}$ = 1713, 1116, 526 cm^{-1}. ^1H NMR ($CDCl_3$): δ = 0.88 (t, *J* = 6.4 Hz, 6 H), 1.11–1.58 (m, 36 H), 1.79 (dt, *J* = 8.0 Hz, *J* = 6.4 Hz, 4 H), 3.97 (t, *J* = 6.6 Hz, 4 H), 6.89 (d, *J* = 8.4 Hz, 4 H), 6.99 (d, *J* = 16.2 Hz, 2 H), 7.12 (d, *J* = 16.0 Hz, 2 H), 7.44 (d, *J* = 8.0 Hz, 4 H), 7.71 (s, 1 H), 8.16 (s, 2 H) ppm. ^{13}C NMR ($CDCl_3$): δ = 159.4, 155.7, 152.0, 150.0, 149.8, 149.4, 149.3, 148.1, 147.8, 147.7, 147.6, 147.3, 146.9, 146.8, 146.6, 146.5, 146.4, 146.3, 146.2, 146.1, 145.9, 145.4, 145.30, 145.0, 144.8, 144.0, 143.1, 143.0, 142.7, 139.7, 139.1, 136.0, 132.8, 132.3, 132.2, 130.3, 129.9, 129.7, 129.5, 129.5, 128.2, 128.1, 127.7, 125.4, 121.4, 115.1, 83.6, 80.0, 68.3, 32.1, 28.9, 26.2, 22.9, 14.3 ppm. UV/Vis (CH_2Cl_2): λ_{max} ($\log\varepsilon$) = 327.0 (4.6), 427.0 nm (3.5). MS (MALDI-TOF): *m/z* = 1411.4 $[M]^+$, 720 $[C_{60}]^+$.

Acknowledgments

Financial support for this work was provided by a grant from the Ministerio de Educación y Ciencia of Spain and the Fondo Europeo de Desarollo Regional (FEDER) (Project CTQ2004-00364/BQU) and the Junta de Comunidades de Castilla-La Mancha (Project PAI-05-068). L. P. acknowledges the receipt of a fellowship from the Ministerio de Educación y Ciencia. This work was also partly supported by a Grant-in-Aid for Scientific Research on Priority Areas (417) from the Ministry of Education, Science, Sports and Culture of Japan. M. E. K. thanks the Japan Society for the Promotion of Science (JSPS).

[1] a) C. J. Brabec, N. S. Sariciftci, J. C. Hummelen, *Adv. Funct. Mater.* **2001**, *11*, 15–26; b) F. Wudl, *J. Mater. Chem.* **2002**, *12*, 1959–1963; c) J.-F. Nierengarten, *Sol. Energy Mater. Sol. Cells* **2004**, *83*, 187–199.

[2] D. Gust, T. A. Moore, A. L. Moore, *Acc. Chem. Res.* **2001**, *34*, 40–48.

[3] A. Hirsch, M. Brettrich, *Fullerenes: Chemistry and Reactions*, Wiley-VCH, Weinheim, **2005**.

[4] L. Echegoyen, L. E. Echegoyen, *Acc. Chem. Res.* **1998**, *31*, 593–601.

[5] a) D. M. Guldi, *Chem. Soc. Rev.* **2002**, *31*, 22–36; b) J. W. Verhoeven, *J. Photochem. Photobiol. C* **2006**, *7*, 40–60.

[6] J. F. Nierengarten, N. Armaroli, G. Accorsi, Y. Rio, J.-F. Eckert, *Chem. Eur. J.* **2003**, *9*, 37–41.

[7] a) J.-F. Eckert, J.-F. Nicoud, J.-F. Nierengarten, S.-G. Liu, L. Echegoyen, F. Barigelletti, N. Armaroli, L. Ouali, V. Krasnikov, G. Hadziioannou, *J. Am. Chem. Soc.* **2000**, *122*, 7467–7479; b) E. Peeters, P. A. van Hal, J. Knol, C. J. Brabec, N. S. Sariciftci, J. C. Hummelen, R. A. J. Janssen, *J. Phys. Chem. B* **2000**, *104*, 10174–10190; c) N. Armaroli, G. Accorsi, J.-P. Gisselbrecht, M. Gross, V. Krasnikov, D. Tsamouras, G. Hadziioannou, M. J. Gómez-Escalonilla, F. Langa, J.-F. Eckert, J.-F. Nierengarten, *J. Mater. Chem.* **2002**, *12*, 2077–2087.

[8] a) N. Armaroli, F. Barigelletti, P. Ceroni, J.-F. Eckert, J.-F. Nicoud, J.-F. Nierengarten, *Chem. Commun.* **2000**, 599–600; b) G. Accorsi, N. Armaroli, J.-F. Eckert, J.-F. Nierengarten, *Tetrahedron Lett.* **2002**, *43*, 65–68.

[9] a) J. L. Segura, R. Gomez, N. Martin, C. P. Luo, A. Swartz, D. M. Guldi, *Chem. Commun.* **2001**, 707–708; b) D. M. Guldi, A. Swartz, C. Luo, R. Gomez, J. L. Segura, N. Martin, *J. Am. Chem. Soc.* **2002**, *124*, 10875–10886.

[10] L. Pérez, J. C. García-Martínez, E. Díez-Barra, P. Atienzar, H. García, J. Rodríguez-López, F. Langa, *Chem. Eur. J.* **2006**, *12*, 5149–5157.

[11] M. Prato, M. Maggini, *Acc. Chem. Res.* **1998**, *31*, 519–526.
[12] a) P. de la Cruz, E. Espíldora, J. J. García, A. de la Hoz, F. Langa, N. Martín, L. Sánchez, *Tetrahedron Lett.* **1999**, *40*, 4889–4892; b) F. Langa, P. de la Cruz, E. Espíldora, A. González-Cortés, A. de la Hoz, V. López-Arza, *J. Org. Chem.* **2000**, *65*, 8675–8684; c) H. Irngartinger, P. W. Fettel, T. Escher, P. Tinnefeld, S. Nord, M. Sauer, *Eur. J. Org. Chem.* **2000**, 455–465; d) B. M. Illescas, N. Martín, *J. Org. Chem.* **2000**, *65*, 5986–5995; e) F. Langa, P. de la Cruz, J. L. Delgado, M. J. Gómez-Escalonilla, A. González-Cortés, A. de la Hoz, V. López-Arza, *New J. Chem.* **2002**, *26*, 76–80.
[13] a) P. de la Cruz, A. Díaz-Ortiz, J. J. García, M. J. Gómez-Escalonilla, A. de la Hoz, F. Langa, *Tetrahedron Lett.* **1999**, *40*, 1587–1590; b) F. Langa, P. de la Cruz, E. Espíldora, A. de la Hoz, J. L. Bourdelande, L. Sánchez, N. Martín, *J. Org. Chem.* **2001**, *66*, 5033–5041.
[14] D. M. Guldi, M. Prato, *Chem. Commun.* **2004**, 2517–2525.
[15] a) F. Langa, M. J. Gómez-Escalonilla, E. Diez-Barra, J. C. García-Martínez, A. de la Hoz, J. Rodríguez-López, A. González-Cortes, V. López-Arza, *Tetrahedron Lett.* **2001**, *42*, 3435–3438; b) J. L. Delgado, P. de la Cruz, V. López-Arza, F. Langa, D. B. Kimball, M. M. Haley, *J. Org. Chem.* **2004**, *69*, 2661–2666; c) F. Langa, M. J. Gómez-Escalonilla, J.-M. Rueff, T. M. Figueira Duarte, J.-F. Nierengarten, V. Palermo, P. Samorì, Y. Rio, G. Accorsi, N. Armaroli, *Chem. Eur. J.* **2005**, *11*, 4405–4415.
[16] J. J. Oviedo, M. E. El-Khouly, P. de la Cruz, L. Pérez, J. Garín, J. Orduna, Y. Araki, F. Langa, O. Ito, *New J. Chem.* **2006**, *30*, 93–101.
[17] a) X. Wang, E. Perzon, J. L. Delgado, P. de la Cruz, F. Zhang, F. Langa, M. Andersson, O. Inganäs, *Appl. Phys. Lett.* **2004**, *85*, 5081–5083; b) X. Wang, E. Perzon, F. Oswald, F. Langa, S. Admassie, M. Andersson, O. Inganäs, *Adv. Funct. Mater.* **2005**, *15*, 1665–1670.
[18] E. Díez-Barra, J. C. García-Martínez, S. Merino, R. del Rey, J. Rodríguez-López, P. Sánchez-Verdú, J. Tejeda, *J. Org. Chem.* **2001**, *66*, 5664–5670.
[19] B. S. Furniss, A. J. Hannaford, P. W. G. Smith, A. R. Tatchell, *Vogel's Textbook of Practical Organic Chemistry*, Wiley, New York, **1989**.
[20] A focused microwave oven from CEM Discovery was used.
[21] D. F. Perepichka, M. R. Bryce, *Angew. Chem. Int. Ed.* **2005**, *44*, 2–5.
[22] A. Honciuc, A. Jaiswal, A. Gong, K. Ashworth, C. W. Spangler, I. R. Peterson, L. R. Dalton, R. M. Metzger, *J. Phys. Chem. B* **2005**, *109*, 857–871.
[23] a) A. Weller, *Z. Phys. Chem. Neue Folge* **1982**, *133*, 93–98; b) D. Rehm, A. Weller, *Ber. Bunsen-Ges. Phys. Chem.* **1969**, *73*, 834–839; c) D. Rehm, A. Weller, *Isr. J. Chem.* **1970**, *8*, 259–271.
[24] a) R. M. Noyes, *J. Am. Chem. Soc.* **1962**, *84*, 513–522; b) J. F. Coetzee, J. J. Camion, *J. Am. Chem. Soc.* **1967**, *89*, 2513–2517; c) S. Fukuzumi, J. K. Kochi, *J. Am. Chem. Soc.* **1982**, *104*, 7599–7609; d) A. Weller, *Z. Phys. Chem.* **1982**, *133*, 93–98.
[25] a) P. A. Liddell, J. P. Sumida, A. N. Macpherson, L. Noss, G. R. Seely, K. N. Clark, A. L. Moore, T. A. Moore, D. Gust, *Photochem. Photobiol.* **1994**, *60*, 537–541; b) P. S. Baran, R. R. Monaco, A. U. Khan, D. I. Schuster, S. R. Wilson, *J. Am. Chem. Soc.* **1997**, *119*, 8363–8364; c) D. M. Guldi, *Chem. Commun.* **2000**, 321–328; d) H. Imahori, M. E. El-Khouly, M. Fujitsuka, O. Ito, Y. Sakata, S. Fukuzumi, *J. Phys. Chem. A* **2001**, *105*, 325–332; e) H. Imahori, D. M. Guldi, K. Tamaki, Y. Yoshida, C. Luo, Y. Sakata, S. Fukuzumi, *J. Am. Chem. Soc.* **2001**, *123*, 6617–6628; f) F. D'Souza, G. R. Deviprasad, M. E. El-Khouly, M. Fujitsuka, O. Ito, *J. Am. Chem. Soc.* **2001**, *123*, 5277–5284; g) S. Fukuzumi, H. Imahori, H. Yamada, M. E. El-Khouly, M. Fujitsuka, O. Ito, *J. Am. Chem. Soc.* **2001**, *123*, 2571–2575; h) H. Imahori, Y. Mori, Y. Matano, *J. Photochem. Photobiol. C: Rev.* **2003**, *4*, 51–83; i) M. E. El-Khouly, O. Ito, P. M. Smith, F. D'Souza, *J. Photochem. Photobiol. C: Rev.* **2004**, *5*, 79–104.
[26] J. L. Delgado, M. E. El-Khouly, Y. Araki, M. J. Gómez-Escalonilla, P. de la Cruz, F. Oswald, O. Ito, F. Langa, *Phys. Chem. Chem. Phys.* **2006**, *8*, 4104–4111.
[27] a) R. A. Marcus, *J. Chem. Phys.* **1956**, *24*, 966–978; R. A. Marcus, *J. Chem. Phys.* **1957**, *26*, 867–871; R. A. Marcus, *J. Chem. Phys.* **1957**, *26*, 872–877; b) R. A. Marcus, *J. Chem. Phys.* **1965**, *43*, 679–701; c) R. A. Marcus, N. Sutin, *Biochim. Biophys. Acta* **1985**, *811*, 265–322.
[28] a) S. D. A. Sandanayaka, K. Matsukawa, T. Ishi-I, S. Mataka, Y. Araki, O. Ito, *J. Phys. Chem. B* **2004**, *108*, 19995–20004; b) H. Luo, M. Fujitsuka, Y. Araki, O. Ito, P. Padmawar, L. Chiang, *J. Phys. Chem. B* **2003**, *107*, 9312–9318.
[29] S. I. Murov, *Handbook of Photochemistry*, Marcel Dekker, New York, **1985**.
[30] Y. Araki, Y. Yasamura, O. Ito, *J. Phys. Chem. B* **2005**, *109*, 9843–9848.
[31] M. J. Frisch, G. W. Trucks, H. B. Schlegel, G. E. Scuseria, M. A. Robb, J. R. Cheeseman, J. A. Montgomery, Jr., T. Vreven, K. N. Kudin, J. C. Burant, J. M. Millam, S. S. Iyengar, J. Tomasi, V. Barone, B. Mennucci, M. Cossi, G. Scalmani, N. Rega, G. A. Petersson, H. Nakatsuji, M. Hada, M. Ehara, K. Toyota, R. Fukuda, J. Hasegawa, M. Ishida, T. Nakajima, Y. Honda, O. Kitao, H. Nakai, M. Klene, X. Li, J. E. Knox, H. P. Hratchian, J. B. Cross, C. Adamo, J. Jaramillo, R. Gomperts, R. E. Stratmann, O. Yazyev, A. J. Austin, R. Cammi, C. Pomelli, J. W. Ochterski, P. Y. Ayala, K. Morokuma, G. A. Voth, P. Salvador, J. J. Dannenberg, V. G. Zakrzewski, S. Dapprich, A. D. Daniels, M. C. Strain, O. Farkas, D. K. Malick, A. D. Rabuck, K. Raghavachari, J. B. Foresman, J. V. Ortiz, Q. Cui, A. G. Baboul, S. Clifford, J. Cioslowski, B. B. Stefanov, G. Liu, A. Liashenko, P. Piskorz, I. Komaromi, R. L. Martin, D. J. Fox, T. Keith, M. A. Al-Laham, C. Y. Peng, A. Nanayakkara, M. Challacombe, P. M. W. Gill, B. Johnson, W. Chen, M. W. Wong, C. Gonzalez, J. A. Pople, *Gaussian 03*, Revision B.04, Gaussian, Inc., Pittsburgh PA, **2003**..
[32] K. E. Larsen, K. B. G. Torssell, *Tetrahedron* **1984**, *40*, 2985–2988.

Received: October 20, 2006
Published Online: March 13, 2007

